

Effect of vanadium deficiency on properties of polycrystalline LaVO_3

S. Jamali Gharetape,¹ M. P. Singh,^{1,a)} F. S. Razavi,¹ D. A. Crandles,¹ L. Y. Zhao,² and K. T. Leung²

¹Department of Physics, Brock University, St. Catharines, Ontario L2S 3A1, Canada

²Department of Chemistry, University of Waterloo, Waterloo, Ontario N2L 3G1, Canada

(Received 27 September 2010; accepted 6 January 2011; published online 2 February 2011)

We report the influence of V deficiency on structure, transport, and magnetic properties of polycrystalline LaVO_3 . Up to 10% V-deficient samples were synthesized using standard solid state chemistry route. Structural and spectroscopic studies show that it intricately modifies lattice parameters and oxidation states of V. Further temperature dependent resistivity data reveal that V deficiency induces an enhancement in the resistivity and activation energy. The paramagnetic moment of these samples depends on net V composition while all samples exhibit a paramagnetic-to-antiferromagnetic transition at about 140 K. These distinct properties are understood owing to the presence of multiple oxidations states of V, predominantly V^{3+} and V^{4+} , in nonstoichiometric LaVO_3 . © 2011 American Institute of Physics. [doi:10.1063/1.3549179]

Renewed interests in V-based perovskite oxides arise owing to the possibility of tuning their properties, such as electric and magnetic through structural modification, chemical doping, and/or pressure.^{1–7} In this respect, various studies have recently been conducted on the bulk and thin film of RVO_3 , wherein R stands for rare earth elements.^{2–9} These studies demonstrate that V, in these systems, is in a 3+ oxidation state and attains a $3d^2(t_{2g}^2 e_g^0)$ electron configuration. Further, these oxides display a strong competing spin-orbit and orbit-lattice interactions that lead to unique magnetic, optical, and electrical properties.^{2,3,8,9} In particular, LaVO_3 goes through an orthorhombic-to-monoclinic transition around 140 K due to the distortion in VO_6 octahedra. Despite the several studies, still the physical properties of orthovanadates are not well understood.^{8–11} For example, the origin of weak ferromagnetism and anomalous magnetic field dependent diamagnetic properties of LaVO_3 are still debatable.^{8–11}

Nonstoichiometry of cations and/or oxygen in perovskite oxides plays a crucial role in provoking a new set of physical properties. This effect has been extensively studied in various perovskite oxides.¹² For example, it is possible to induce ferromagnetic and colossal magnetoresistance behavior in LaMnO_3 through La/Mn/O nonstoichiometry.¹² Thus, one may expect that the cationic deficiency in LVO may also alter its properties. In this context, Fjellvag and co-workers^{13,14} studied the influence of La deficiency up to 10% on the structural and physical properties of LVO. They reported that La deficiency significantly alters the lattice parameters while all samples adopt the orthorhombic crystal symmetry at 300 K. Neutron scattering studies¹⁴ on LaVO_3 and $\text{La}_{0.92}\text{VO}_3$ show that they undergo a first order structural transition at 140 and 82 K, respectively, and possess C-type antiferromagnetism. However, no structural transition and no long range magnetic ordering were observed for $\text{La}_{0.9}\text{VO}_3$. Further, the impact of oxygen composition on the structure and properties of LVO are studied.^{15,16} These studies also show that such changes intricately modify its behavior.

Unlike the La deficiency, very little is known about the effect of V deficiency on the structural and physical proper-

ties of LVO. In this paper, we report the structural, magnetic, and transport properties of V-deficient LVO. The vanadium deficient LaV_xO_3 (viz., $x=1.0, 0.98, 0.96, 0.94, 0.92$) polycrystalline samples were synthesized in two steps via standard solid state chemistry routes. Appropriate stoichiometric amounts of La_2O_3 and V_2O_5 powders were mixed using mortar and pestle and ultimately pressed in form of pellets. To remove the carbonate and/or hydrate formation, La_2O_3 was precalcined at 950 °C for 2 h in air. The pellets were subjected to sintering at 950 °C in flowing He/ H_2 (5%) ambient for 2 h. They were reground and pressed in form of pellets. In the final step, these pellets were annealed at 1100 °C for 30 h in He/ H_2 (8.5%). Attention was paid to obtain the oxygen stoichiometric samples. X-ray photoelectron spectroscopy (XPS) measurements were performed using a Thermo-VG Scientific ESCALab 250 microprobe equipped with a monochromatic Al $K\alpha$ x-ray source. C 1s core-level spectra were used as an internal standard. Temperature and magnetic field dependence of magnetization were measured using a superconducting quantum interferometer device magnetometer from Quantum Design. Transport properties were measured in four-probe configuration using a custom built system.

Past studies show that LaVO_3 adopts orthorhombic crystal symmetry¹¹ at 300 K with lattice parameters of $a=5.55548 \text{ \AA}$, $b=5.55349 \text{ \AA}$, and $c=7.84868 \text{ \AA}$. Crystallinity and phase formation of our samples were studied using a Philips x-ray diffractometer (XRD) equipped with a Cu $K\alpha$ source. Figure 1(a) presents typical XRD patterns of the LaV_xO_3 samples. Reflections are indexed based on orthorhombic $Pbnm$ symmetry. The absence of any unaccountable reflection in the XRD patterns confirms that samples are homogenous and free from impurity phases. It is important to note that all samples, irrespective of V deficiency, exhibit the orthorhombic crystal symmetry and the cations have the same coordination. Compared to stoichiometric LVO, XRD data analysis also reveals that V-deficiency modifies the lattice parameters of LVO. For example, the c-lattice parameter of LaVO_3 is 7.842 Å, while its value is about 7.944 Å in $\text{LaV}_{0.92}\text{O}_3$ leading to 1.3% enhancement in its value as a result of V-deficiency. A similar subtle trend is also noticed in a- and b-lattice parameters.

^{a)}Electronic mail: mangala.singh@brocku.ca.

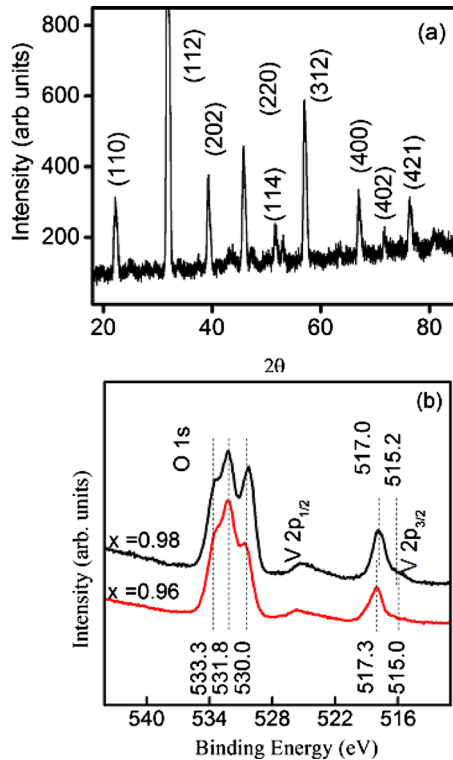


FIG. 1. (Color online) (a) Typical θ - 2θ XRD pattern of $\text{LaV}_{0.94}\text{O}_3$. (b) Typical core-level XPS spectra of V $2p$ and O $1s$ in samples containing 0.98 and 0.96 V composition. Dotted lines are only to give the idea about the different peak positions and asymmetry in the spectra.

To examine the chemical nature of La, V, and/or O in our samples get a deeper insight, XPS study was carried out. Figure 1(b) presents typical core-level XPS spectra of O $1s$ and V $2p$ collected on two samples, viz., $x=0.98$ and 0.95. Irrespective of V composition, core-level V $2p_{3/2}$ spectra are asymmetric. Further, its peak position relatively shifts toward higher binding energy, revealing that the average oxidation state of V increases from 3+ to a higher oxidation state in deficient samples.¹⁷ The binding energy positions of V, extracted from the multiple peak fit to V ($2p_{3/2}$) core-level spectra (not shown here), are 515.2 and 517.0 eV in the 0.98 sample, whereas in the 0.96 sample these corresponding values are 515.0 and 517.3 eV. These values show that V^{3+} (515.0–515.2 eV) and V^{4+} (517.0–517.3 eV) are present in our samples and discernible changes in the relative compositions follow the trend in the V stoichiometry in LVO.¹⁷ The presence of multiple oxidation states of V is further confirmed by core-level spectra of O $1s$ [see Fig. 1(b)]. A close inspection of core-level O $1s$ spectra reveals the presence of three discernible peaks (at 530.0, 531.8, and 533.3 eV), indicating that oxygen is in different chemical environments. The peak profile of the O $1s$ feature and its connection to possible asymmetric overlap of electronic wave functions of V and O in the deficient samples require further investigation and our detailed results will be reported elsewhere. Nonetheless, the presence of V^{2+} , due to the possible excessive reduction, can also be ruled out because of the absence of features at lower binding energy (below 514.5 eV) in our samples.¹⁷ Thus, XPS studies demonstrate that V is present in multiple oxidation states and can be assigned to V^{3+} and V^{4+} . The composition of V^{4+} increases with a progressive decrease in V composition.

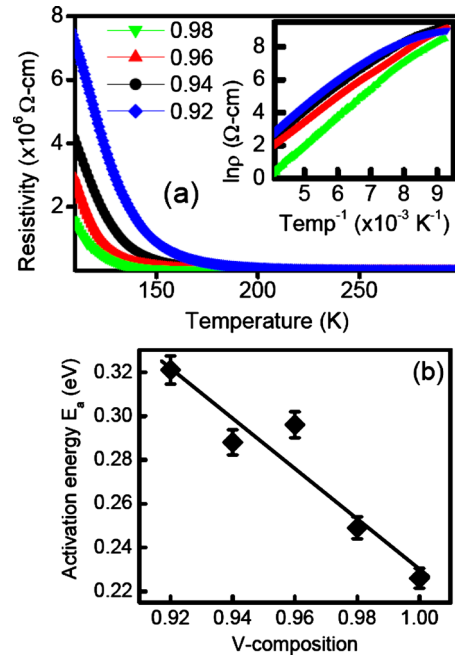


FIG. 2. (Color online) (a) Temperature dependent resistivity of samples containing different stoichiometry of V. (b) Variation of thermal activation energy as a function of stoichiometry of V. The inset of (b) presents $\ln \rho$ vs $1/T$ curve. The solid line in (b) is just a guide for the eye.

Temperature dependent resistivity (i.e., ρ -T) curves of various samples are plotted in Fig. 2. Two important features can be noted: (i) As samples were cooled down, resistivity increases, revealing that they exhibit an insulator behavior. (ii) With a progressive decrease in the V stoichiometry, the resistivity increases drastically. In a simple scenario, the resistivity of a given materials depends on the total number of charge carriers, the amplitude of the electron-phonon interaction, and the concentrations of defect sites that act as potential scattering centers for the current-carrying charge carriers. The V deficiency is critical owing to the role of V–O–V bonds in the electrical conduction process. Further, V deficiency partially changes the oxidation state of $\text{V}^{3+}(3d^2)$ to $\text{V}^{4+}(3d^1)$ to neutralize the system, as confirmed by XPS study. Although this enhancement in the oxidation state of vanadium generates the holes in our samples, the presence of defect states localize the charge carriers.¹⁻⁴ The delocalization of charge carriers are further hindered by the absence of V in the lattices which randomly decouples the overlap of V–O–V wave functions. This shows that V stoichiometry plays a decisive role in determining its electrical properties.

In Mott insulators with intrinsic defects, electrical conduction may be described through a thermally activated process and/or variable range hopping process.¹⁸ In thermally activated process, $\rho(T)$ describes as $\rho_0 \exp(E_a/2k_B T)$, where ρ_0 is the residual resistivity, E_a is thermal activation energy, k_B is the Boltzmann constant, and T is the temperature. Using the ρ -T curves, we extracted the value of E_a and it is plotted as a function of V composition in Fig. 2(b). Interestingly, the value of E_a increases with a decrease in the V stoichiometry. This illustrates that the carriers are localized. Within the temperature limit of this work, our results show that the conduction process is thermally activated.

Zero-field cooled temperature dependence magnetization (M-T) curves are plotted in Fig. 3. Irrespective of the V composition, M-T curves of all the samples show a peak

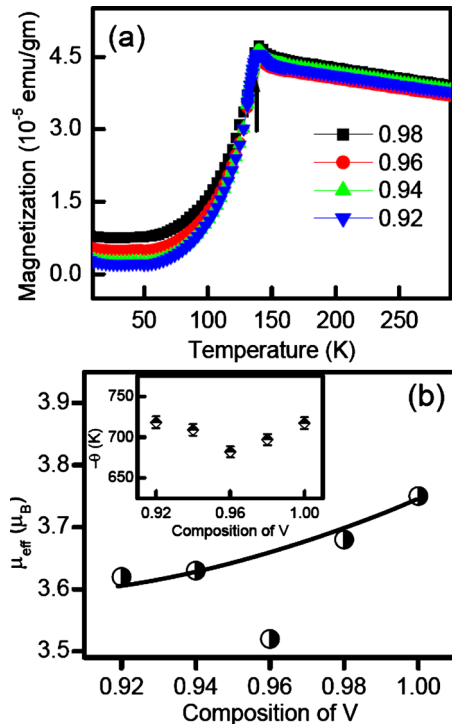


FIG. 3. (Color online) (a) Zero-field cooled M-T curves and (b) variation in the value of μ_{eff} as a function of V stoichiometry. The inset of (b) presents variation in the value of Weiss temperature (θ) as a function of V stoichiometry in the samples. The solid line in (b) is just a guide to the eye and the arrow in (a) shows paramagnetic-to-antiferromagnetic transition point.

formation at around 140 K, revealing the antiferromagnetic-to-paramagnetic transition (T_N). This indicates that these samples are antiferromagnetic. Similar effects are also observed on the other nonstoichiometric perovskites, such as Mn-deficient LaMnO_3 .¹⁶ Surprisingly, the value of T_N is identical for all V-deficient samples. On the contrary, a significant decrease in the value of T_N was observed as a function of La deficiency in La-deficient samples.^{13,14} Taking into account the electrical properties, this possibly can be understood as follows: It is important to note that V–O bond is ultimately responsible for magnetic behavior in LVO. The doping of divalent cations at La site (e.g., Sr or Ca) (Ref. 4) in LVO promotes the enhancement in oxidation states of V, as seen in V-deficient samples. This increases the charge carrier concentrations through the creation of holes. Since the V–O–V bonds are intact in such samples, they ultimately lead to a paramagnetic metallic behavior in doped LVO owing to band filling process. However, such an increase in the bandwidth is hindered in vanadium-deficient samples due to localized states created by the defects and random-absence of V–O bonds in the lattice due to the V vacancies. Thus, the magnetic and transport properties of our samples are consistent with their structural behaviors.

A closer inspection of the M-T curves below 50 K shows a systematic decrease in the value of magnetization of LVO samples as one reduces the V composition. Further above T_N , all samples follow the Curie–Weiss law and M-T data were fitted to this law to extract the value of paramagnetic moment μ_{eff} and Weiss temperature Θ [Fig. 3(b)]. This analysis reveals that V deficiency induces a reduction in the value of paramagnetic moment, which can be understood by taking into account the multiple oxidation states of V (viz., V^{3+} and V^{4+}) and the ratio of their concentrations in our

samples. Irrespective of the V composition, all samples have a negative value of Θ confirming that they are antiferromagnetic. This reveals that V deficiency does not destroy the long range antiferromagnetic ordering in LVO. In contrast, La-deficient samples¹⁴ show no net change in the value of μ_{eff} as a function of La nonstoichiometry, and follow the identical trend, as seen in our samples, in the value of Θ . Further, the value of μ_{eff} is larger than the expected value of spin-only V magnetic moments, suggesting that partial contributions arise from the orbital moment as demonstrated by various researchers in the past.^{2–9}

In summary, we studied the impact of V deficiency on the properties of LaVO_3 . It demonstrates that the V deficiency induces multiple oxidation state of V and plays a decisive role in determining its physical properties. Further, antiferromagnetic ordering is found to be robust in V-deficient LaVO_3 .

This work was supported by the Natural Sciences and Engineering Research Council (Canada), Canadian Foundation for Innovation (CFI), Ontario Ministry of Research and Innovation (MRI), and Brock University.

¹T. Higuchi, Y. Hotta, T. Susaki, A. Fujimori, and H. Y. Hwang, *Phys. Rev. B* **79**, 075415 (2009); J. B. Goodenough, *Rep. Prog. Phys.* **67**, 1915 (2004).

²U. Lüders, W. C. Sheets, A. David, W. Prellier, and R. Fesard, *Phys. Rev. B* **80**, 241102 (2009); H. Weng and K. Terakura, *ibid.* **82**, 115105 (2010); M. Takizawa, Y. Hotta, T. Susaki, Y. Ishida, H. Wadati, Y. Takata, K. Horiba, M. Matsunami, S. Shin, M. Yabashi, K. Tamasaku, Y. Nishino, T. Ishikawa, A. Fujimori, and H. Y. Hwang, *Phys. Rev. Lett.* **102**, 236401 (2009).

³Y. Ren, T. T. M. Palstra, D. I. Khomskii, E. Pellegrin, A. A. Nugroho, A. A. Menovsky, and G. A. Sawatzky, *Nature (London)* **396**, 441 (1998); F. Inaba, T. Arima, T. Ishikawa, T. Katsufuji, and Y. Tokura, *Phys. Rev. B* **52**, R2221 (1995).

⁴M. H. Sage, G. R. Blake, and T. T. M. Palstra, *Phys. Rev. B* **77**, 155121 (2008); I. V. Solovyev, *ibid.* **74**, 054412 (2006).

⁵G. Khaliullin, P. Horsch, and A. M. Oles, *Phys. Rev. Lett.* **86**, 3879 (2001).

⁶J. S. Zhou, J. B. Goodenough, J. Q. Yan, and Y. Ren, *Phys. Rev. Lett.* **99**, 156401 (2007).

⁷Y. Hotta, Y. Mukunoki, T. Susaki, H. Y. Hwang, L. Fitting, and D. A. Muller, *Appl. Phys. Lett.* **89**, 031918 (2006); W. Choi and T. Sands, *J. Mater. Res.* **15**, 1 (2000).

⁸H. C. Nguyen and J. B. Goodenough, *Phys. Rev. B* **52**, 324 (1995).

⁹A. V. Mahajan, D. C. Johnston, D. R. Torgeson, and F. Borsa, *Phys. Rev. B* **46**, 10966 (1992).

¹⁰S. Yoon, *J. Appl. Phys.* **105**, 07D509 (2009).

¹¹P. Bordet, C. Chailout, M. Marezio, Q. Huang, A. Santoro, S. W. Cheong, H. Takagi, C. S. Oglesby, and B. Batlogg, *J. Solid State Chem.* **106**, 253 (1993).

¹²*Colossal Magneto-Resistance, Charge Ordering, and Related Properties of Rare Earth Manganese Oxides*, edited by C. N. R. Rao and B. Raveau (World Scientific, Singapore, 1998).

¹³H. Seim and H. Fjellvag, *Acta Chem. Scand.* **52**, 1096 (1998).

¹⁴H. Seim, H. Fjellvag, and B. C. Hauback, *Acta Chem. Scand.* **52**, 1301 (1998).

¹⁵N. H. Hur, S. H. Kim, K. S. Yu, Y. K. Park, J. C. Park, and S. J. Kim, *Solid State Commun.* **92**, 541 (1994); P. Antoine, R. Assabaa, P. L'Haridon, R. Marchand, Y. Laurent, C. Michel, and B. Raveau, *Mater. Sci. Eng., B* **5**, 43 (1989).

¹⁶J. Topfer and J. B. Goodenough, *J. Solid State Chem.* **130**, 117 (1997); I. O. Troyanchuk, V. A. Khomchenko, M. Tovar, H. Szymczak, and K. Barner, *Acta Phys. Pol. A* **105**, 27 (2004).

¹⁷J. Mendiola, R. Casanova, and Y. Barbaux, *J. Electron Spectrosc. Relat. Phenom.* **71**, 249 (1995); D. Briggs and M. P. Seah, *Practical Surface Analysis* (Wiley, New York, 1990), Vol. 1.

¹⁸P. A. Cox, *Transition Metal Oxides: An Introduction to Their Electronic Structure and Properties* (Oxford University Press, United Kingdom, 1992).